

Lawrence Berkeley National Laboratory

Recent Work

Title

ON THE MECHANISM OF ANODIC CHLORATE FORMATION IN DILUTE NaCl SOLUTIONS

Permalink

<https://escholarship.org/uc/item/59x598pf>

Authors

Ibl, N.

Landolt, D.

Publication Date

1967-11-01

C.L.

University of California

Ernest O. Lawrence Radiation Laboratory

ON THE MECHANISM OF ANODIC CHLORATE
FORMATION IN DILUTE NaCl SOLUTIONS

N. Ibl and D. Landolt

November 1967

RECEIVED
LAWRENCE
RADIATION
LIBRARY
DOCUMENT

TWO-WEEK LOAN COPY

*This is a Library Circulating Copy
which may be borrowed for two weeks.
For a personal retention copy, call
Tech. Info. Division, Ext. 5545*

*UCRL-17461
C.L.*

DISCLAIMER

This document was prepared as an account of work sponsored by the United States Government. While this document is believed to contain correct information, neither the United States Government nor any agency thereof, nor the Regents of the University of California, nor any of their employees, makes any warranty, express or implied, or assumes any legal responsibility for the accuracy, completeness, or usefulness of any information, apparatus, product, or process disclosed, or represents that its use would not infringe privately owned rights. Reference herein to any specific commercial product, process, or service by its trade name, trademark, manufacturer, or otherwise, does not necessarily constitute or imply its endorsement, recommendation, or favoring by the United States Government or any agency thereof, or the Regents of the University of California. The views and opinions of authors expressed herein do not necessarily state or reflect those of the United States Government or any agency thereof or the Regents of the University of California.

Submitted to Journal of the
Electrochemical Society

UCRL-17461
Preprint

UNIVERSITY OF CALIFORNIA
Lawrence Radiation Laboratory,
Berkeley, California
AEC Contract No. W-7405-eng-48

ON THE MECHANISM OF ANODIC CHLORATE
FORMATION IN DILUTE NaCl SOLUTIONS

N. Ibl and D. Landolt

November 1967

ON THE MECHANISM OF ANODIC CHLORATE
FORMATION IN DILUTE NaCl SOLUTIONS

N. Ibl and D. Landolt[†]

Department of Industrial and Engineering Chemistry,
Swiss Federal Institute of Technology, Zurich, Switzerland

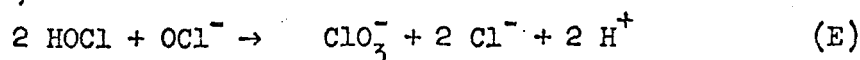
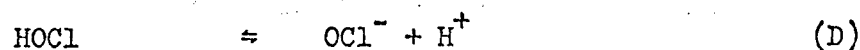
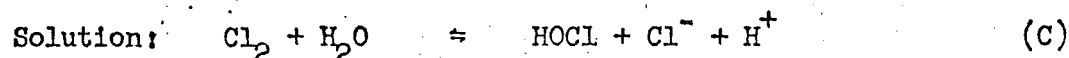
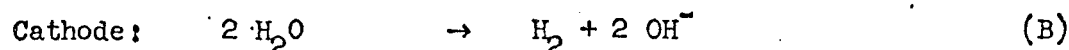
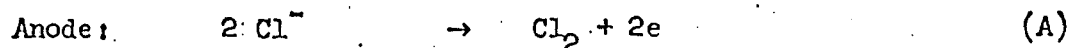
ABSTRACT

The rates of anodic chlorate formation were measured under a variety of well defined hydrodynamic conditions. In dilute NaCl solutions (<0.1 M) these rates are up to 60 times larger than those calculated for mass transport control as hitherto postulated.

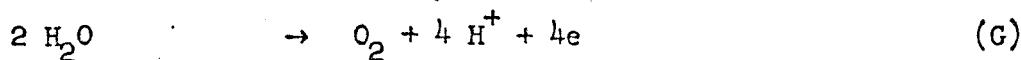
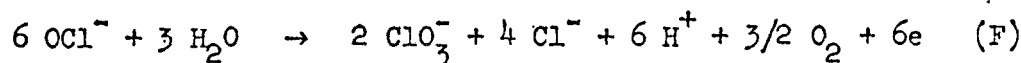
The rates of chlorate formation were calculated using a model which involves the coupling of mass transfer with a chemical reaction (chlorine hydrolysis) proceeding in the diffusion layer. The agreement between the calculated and the experimental values is satisfactory. The model used describes adequately the mechanism of anodic chlorate formation in the range of conditions investigated: In dilute NaCl solutions the rate of chlorate formation is governed by the kinetics of the chlorine hydrolysis. At higher chloride concentrations equilibrium may limit the hydrolysis and the mechanism of the process then changes accordingly.

I. INTRODUCTION: PRELIMINARY EXPERIMENTS

Chlorate is manufactured industrially by electrolysis of neutral sodium chloride solutions in cells without a diaphragm. The reactions taking place in a chlorate cell were formulated by Foerster and Mueller^{1,2} as follows:



Anodic loss reactions:*



Reaction (G) plays a minor role, as long as the solution does not become too alkaline, or the chloride concentration too low.** According to reactions (E) and (F) chlorate may be formed in two ways, either by a purely chemical reaction of the hypochlorite ion with hypochlorous acid in the bulk solution (chemical chlorate formation) or by electrochemical oxidation of the hypochlorite at the anode under simultaneous oxygen

† Present address: Lawrence Radiation Laboratory, University of California, Berkeley, California, USA.

* Loss reactions at the cathode may be suppressed almost entirely by adding small amounts of potassium bichromate to the solution (Reference 3).

** Formation of perchlorate is another possible anodic loss reaction. It may occur at platinum electrodes but under extreme conditions only.

evolution (anodic chlorate formation). If all chlorate is formed by the chemical reaction (E), six Faradays are consumed in the oxidation of one mole chloride to chlorate. This is said to correspond to a maximum current efficiency τ_{ClO_3} of 100%. If all chlorate is formed by reaction (F) the current efficiency cannot be higher than 66.7% since one third of the current is used for the evolution of oxygen.

Only little is known about the rate determining step of the anodic loss reaction (F) which limits the current efficiency in technical cells. As was already observed by Foerster² the concentration of hypochlorite in the bulk solution increases during electrolysis until a steady state is reached (see Fig. 2). According to this author there is approximate proportionality between the rate of oxygen evolution resulting from reaction (F) and the hypochlorite concentration in the solution, both for the steady and the unsteady state.² This was confirmed later by Knibbs and Palfreeman.⁴ From a discussion of Foerster's results, de Valera⁵ and Beck⁶ concluded that the anodic chlorate formation is controlled by the mass transport of the hypochlorite from the bulk solution toward the anode. In his treatment of Foerster's data, Beck took into account the complication that under transport control the rate of chlorate formation and therefore the rate of oxygen evolution should increase somewhat faster than would correspond to proportionality with the hypochlorite concentration, because the thickness of the diffusion layer decreases when the stirring by the gas bubbles becomes stronger owing to a faster gas evolution. Whereas Foerster worked mainly with platinum electrodes, Hammar and Wranglén⁷ have recently made a comprehensive study of the rate of oxygen evolution in chlorate electrolysis with graphite

electrodes. They also found that the rate of oxygen evolution is proportional to the hypochlorite concentration if the influence of the gas bubbling on δ is taken into account, and they concluded that mass transport of the hypochlorite is the rate determining step of the anodic chlorate formation.

Most of the afore-mentioned experiments of the literature were carried out with concentrated NaCl solutions (>1 M). Recently, Selvig and Ibl made measurements in dilute solutions where the rates of chlorate formation were up to ten times larger than those expected for a diffusion controlled process.⁸ The latter values were calculated from the measured oxygen evolution rate by means of the following correlation for mass transfer at gas evolving electrodes, given by Ibl and Venczel:^{9,11}

$$k_L = \frac{D V^{0.5}}{1.50 \times 10^{-3}}$$

where k_L = mass transfer coefficient (cm/sec); D = diffusion coefficient (cm²/sec); V = gas evolution rate (cm³/cm² min).

Electrolysing acid sodium chloride solutions of various concentrations, Selvig found a strong dependence of the steady state hypochlorite concentration on the chloride concentration. Figure 1 shows results similar to those of Selvig, but obtained in slightly alkaline solutions.¹⁰ Steady state hypochlorite concentrations and chlorate formation rates are given for a variety of experiments performed by electrolysing sodium chloride solutions of various concentrations at constant current density in the absence of forced convection.* Bichromate was added to the

* The cell was constructed in a way to allow circulation of the electrolyte for good mixing. It contained two graphite electrodes (AGLX 58, Union Carbide) of 100 cm² surface area. The electrolyte volume was between 170 and 200 ml.

solution to reduce cathodic losses. pH and chloride concentration were kept constant by adding conc. HCl or NaOH during the experiments. Hypochlorite and chlorate concentrations were followed over time by potentiometric titration (see below). Oxygen and hydrogen evolution rates in the steady state were measured using a standard oxygen absorption method.

The history of a typical experiment is shown in Fig. 2. Starting with no hypochlorite in the solution hypochlorite is built up in the bulk at the beginning of the experiment. Gradually more chlorate is formed until a steady state is reached after some time when hypochlorite concentration and chlorate formation rate remain constant. The steady state values given in Fig. 1 in function of the NaCl concentration show a sharp decrease in the hypochlorite concentration at chloride concentrations below about 400 mM/lit. On the other hand, the chlorate formation rate decreases only slightly, the decrease being possibly due to increased oxygen evolution according to reaction (G).

All the experiments of the literature mentioned so far were carried out without external stirring, the only convection present being that due to gas evolution and to the density differences in the solution. The hydrodynamic conditions were thus not well defined, and an accurate comparison with theoretical relationships is therefore difficult. This also applies to Selvig's results. However, in the latter case the discrepancy with the values calculated for mass transport control are so large that at least under the conditions of Selvig's experiments, the rate of chlorate formation can hardly be interpreted in terms of mass transport alone. Furthermore, the results of Fig. 1 (i.e. the large difference between the steady state hypochlorite concentration measured

in dilute and concentrated NaCl solutions in spite of the almost unchanged rate of chlorate formation) strongly suggest that the kinetics of chlorate formation are more complicated than would correspond to a simple transport mechanism. In the mass transfer theory of chlorate formation, as hitherto developed in the literature, only the diffusion of the hypochlorite toward the anode is considered, without taking into account the possible influence of the kinetics of the hypochlorite formation, i.e. it is more or less tacitly assumed that the chlorine hydrolysis (reaction C) does not take place in the diffusion layer but only in the bulk solution and does not affect the rate of the anodic chlorate formation. However, as we have pointed out in an earlier paper,¹¹ the chlorine hydrolysis is a relatively fast reaction: One should therefore expect that it takes place within the diffusion layer, close to the anode where the chlorine is generated. In the next section the rate of chlorate formation will be calculated using a model which involves the coupling of mass transfer with a chemical reaction (chlorine hydrolysis) in the diffusion layer, and in Section VI the computed values will be compared with measurements carried out under well defined hydrodynamic conditions.

II. THEORETICAL

Schematic concentration profiles near the anode as they may be expected according to the reactions (A) and (F) are shown in Fig. 3; chloride and hypochlorite* are consumed at the anode and must therefore be transported towards it. Molecular chlorine and hydrogen ions are generated and must be transported away from the anode.

The differential equations describing the system are obtained from a balance of mass for an infinitely small volume element in the diffusion layer. Neglecting migration we may write the general equation:

$$\frac{\partial c_1}{\partial t} = -Uv c_1 + D_1 \nabla^2 c_1 + R_1 \quad (1)$$

where: c_1 = concentration of species 1 (M/cm^3) where $i = 1$ stands for molecular chlorine, $i = 2$ for hydrogen ion, $i = 3$ for hypochlorite (sum of hypochlorite ions and hypochlorous acid); t = time (sec); U = velocity vector (cm/sec); D_1 = diffusion coefficient of species 1 (cm^2/sec); R_1 = rate of production of species 1 by chemical reaction ($M/cm^3 \text{ sec}$).

In applying Eq. (1) to our system, the following simplifications were made: The steady state only ($\partial c/\partial t = 0$) was considered. The concept of a stagnant diffusion layer was used, thereby dropping the convection term and only considering the dimension perpendicular to the electrode. The chlorine hydrolysis was treated as a first order

* It is assumed that the dissociation equilibrium of the hypochlorous acid is established infinitely fast and the term hypochlorite is used here as the sum of hypochlorous acid and hypochlorite ions.

irreversible reaction following the rate law:

$$- \frac{dc_1}{dt} = kc_1$$

The differential equation for the chlorine profile in the diffusion layer thus becomes:

$$D_1 \frac{d^2 c_1}{dx^2} - kc_1 = 0 \quad (2)$$

Boundary conditions are: $x = 0$; $D_1 (dc_1/dx) = -i \phi_1 / 2F$; and $x = \delta$, $c_1 = 0$. The first boundary condition states that the chlorine flux at the anode surface is proportional to the density of the current used for the oxidation of chloride ions to chlorine ($\phi_1 =$ fraction of total current used for reaction A). The second boundary condition states that the chlorine concentration in the bulk is essentially zero as it may be expected if the solution is neutral. Equation (2) was first applied to the calculation of the chlorine profile at the anode by Beck.¹² Its solution may be expressed as an exponential function:*

* The exact solution of Eq. (2) is:

$$c_1 = \frac{i \phi_1}{2FD_1 a} \left(\frac{e^{-ax}}{1+e^{-2a\delta}} - \frac{e^{-ax}}{1+e^{2a\delta}} \right) \quad (3')$$

which for $a\delta \gg 1$ takes the form of Eq. (3). The assumption $a\delta > 1$ must be made anyhow if the convection term of the fundamental differential Eq. (1) is to be neglected in the integration.

$$c_1 = \frac{i \phi_1}{2FD_1 a} \exp(-ax) \text{ with } a = \sqrt{\frac{k}{D_1}} \quad (3)$$

Equation (3) holds for the case where the thickness of the layer in which the chemical reaction occurs, is small as compared with the thickness δ which the diffusion layer would have under the same hydrodynamic conditions but without a concomitant chemical reaction. Hydrogen ion and hypochlorite concentration profiles are calculated by integrating the equations:

$$D_2 \frac{d^2 c_2}{dx^2} + kc_1(x) = 0 \quad (4)$$

$$D_3 \frac{d^2 c_3}{dx^2} + kc_1(x) = 0 \quad (5)$$

in which $c_1(x)$ can be expressed by means of Eq. (3). Equation (4) implies that all the hydrogen ions generated in the diffusion layer result from reaction (C), i.e. that no hydrogen ions are produced by reaction (D). This is a reasonable assumption since in the present model the diffusion layer is quite acid (see below) and the dissociation constant¹³ of HClO is 4×10^{-8} moles/lit at 25°C, so that all the hypochlorite is virtually present as HClO in the diffusion layer. Boundary conditions for Eq. (4) are $D_2(dc_2/dx) = i \phi_2/F$ at $x = 0$ and $c_2 = 0$ at $x = \delta$. The flux of the hydrogen ions at the anode surface is given by the density of current corresponding to the evolution of oxygen according to reactions (F) and (G) (ϕ_2 = fraction of total current used for oxygen evolution).^{*} For a neutral solution the hydrogen ion

* The boundary condition at the interface implies the validity of the stoichiometry of the anodic chlorate formation given by reaction (F). This question will be discussed in section V.

concentration in the bulk solution is virtually zero. Boundary conditions for Eq. (5) are: $c_3 = 0$ at $x = 0$ and $c_3 = c_0$ at $x = \delta$. Outside the diffusion layer the hypochlorite concentration equals the bulk concentration which may be determined experimentally. The hypochlorite concentration at the interface is taken as zero, i.e. it is assumed that it is oxidized at the limiting rate. At potentials where Cl^- is discharged this assumption appears justified since various authors^{2,4} have reported that hypochlorite reacts at substantially less positive potentials than Cl^- .

The corresponding solutions of Eqs. (4) and (5), describing the concentration profiles of hydrogen ion and hypochlorite in the diffusion layer, are:

$$c_2 = \frac{i \phi_1}{2FD_2 a} (e^{-a\delta} - e^{-ax}) + \frac{i(\delta-x)}{FD_2} \left(\frac{\phi_1}{2} + \phi_2 \right) \quad (6)$$

$$c_3 = \frac{i \phi_1}{2FD_3 a} (1 - e^{-ax}) + \frac{x}{\delta} \left\{ c_0 - \frac{i \phi_1}{2FD_3 a} (1 - e^{-a\delta}) \right\} \quad (7)$$

The hypochlorite flux at the anode, which corresponds to the rate of anodic chlorate formation, is obtained by differentiating Eq. (7) at $x = 0$:

$$j_h = -D_3 \left(\frac{dc_3}{dx} \right)_{x=0} = \frac{i \phi_1}{2F} \left(\frac{1}{a\delta} - 1 \right) - D_3 \frac{c_0}{\delta} - \frac{i \phi_1}{2Fa\delta} e^{-a\delta} \quad (8)$$

The above calculations show that the chlorine hydrolysis proceeding within the diffusion layer has two consequences: (i) the pH in the diffusion layer, being already lower than that of the bulk solution due to the electrochemical hydrogen ion generation by reaction (F) and (G), is lowered even further by the chemical reaction as may be verified

by comparing the hydrogen ion concentration at the anode surface calculated by Eq. (6) with that expected for a diffusion controlled process according to:

$$(c_2)_{x=0} = \frac{i \phi_2 \delta}{D_2 F} \quad (6')$$

To illustrate the increased acidity of the diffusion layer we calculate from Eq. (6) the concentration of the H^+ ions at the interface for the conditions of the experiment B indicated in Table III. With $k = 6.3 \text{ s}^{-1}$; $D_1 = 10^{-5} \text{ cm}^2 \text{ s}^{-1}$ and $D_2 = 5 \times 10^{-5} \text{ cm}^2 \text{ s}^{-1}$ we obtain $(c_2)_{x=0} = 2.65 \times 10^{-2}$ moles/lit. If we make the corresponding calculation with Eq. (6'), i.e. without taking hydrolysis into account, we get $(c_2)_{x=0} = 1.83 \times 10^{-2}$ moles/lit.

(ii) The concentration gradient of hypochlorite at the anode is increased [Eq. (8)] and hence the rate of anodic chlorate formation becomes higher than expected for a process controlled by diffusion alone.

The shape of the hypochlorite concentration profile in the stagnant diffusion layer is illustrated in Fig. 4. Curve 1 in Fig. 4 was calculated from Eq. (7) for the data of experiment B (Fig. 2) which are given in Table III. The values of the diffusion coefficients of chlorine and hypochlorite were assumed as $10^{-5} \text{ cm}^2/\text{s}$; the rate constant of the chlorine hydrolysis at 13°C was obtained by interpolation of literature values¹⁴ as 6.3 s^{-1} . The dotted line in Fig. 4 represents the concentration profile for a diffusion controlled process. It follows from the two curves that the hypochlorite concentration in the diffusion layer is shifted upwards by the chemical reaction and a steeper concentration gradient at the anode results. Curve 2 illustrates the interesting fact that the concentration in the diffusion layer may even exceed the

bulk concentration. It was calculated in the same way as curve 1 but under the assumption of zero bulk hypochlorite concentration. The concentration maximum within the diffusion layer may be interpreted in such a way that in the absence of hypochlorite in the bulk solution part of the hypochlorite generated within the diffusion layer reacts at the anode and part of it diffuses towards the bulk. In the absence of hypochlorite losses in the bulk curve 2 does not represent a true steady state, because the bulk concentration increases with time. The steady state approach is appropriate, however, for large bulk volumes, where the hypochlorite concentration changes only very slowly. In the absence of hypochlorite losses other than anodic, a true steady state would be reached when the bulk hypochlorite concentration reaches a value equal to the corresponding maximum concentration in the diffusion layer.

In order to test the above ideas about the mechanism of anodic chlorate formation, chlorate formation rates were measured under well defined conditions of hydrodynamic flow, of pH and of temperature.

III. EXPERIMENTAL PROCEDURE AND APPARATUS

The experimental set-up is shown schematically in Fig. 5a. The electrolyte was pumped continuously through a channel cell at flow rates between 10 and 160 cm/sec. The plexiglass cell (Fig. 5b) contained compact impregnated graphite electrodes (EK 200 Ringsdorff, Germany) with smooth surfaces of a length (in the direction of flow) of 5, 10 or 20 cm, the breadth being 5 cm in all cases. A diaphragm (porous polyethylene) could be inserted between anode and cathode. The distance between anode and cathode (or diaphragm) was 2.25 or 9 mm. Potentials at the anode were measured versus a saturated calomel electrode using a backside capillary drilled through the graphite. If a diaphragm was inserted in the cell, the cathodically evolved hydrogen could escape from a glass tube connected to a mercury valve. The temperature of the system was kept low by means of a cryostat in order to suppress the chemical chlorate formation (reaction E). Most experiments were performed at a constant temperature of $7 \pm 0.5^\circ\text{C}$. The pH of the electrolyte was measured with a glass electrode. It was kept constant by automatically adding conc. NaOH or conc. HCl with the help of an "Impulsomat" (Metrohm, Herisau, Switzerland). The flow rate was measured with a rotameter and regulated by two PVC valves and a bypass. A nonpulsating ceramic pump was used (Chemiepumpenbau, Zofingen, Switzerland). The flow of the solution was quieted by passing through 20 to 80 channels, 2 mm in diameter, drilled through plexiglass block S. The whole system contained no metallic parts in contact with the electrolyte. The electrolyte volume used varied from 1.6 to 2.0 lt. The electrolysis was performed at constant

current density, usually 5 mA/cm^2 .^{*} The absence of chemical chlorate formation during the experiments was confirmed by circulating hypochlorite solutions in the flow system under the same conditions, but in the absence of current and measuring hypochlorite and chlorate concentrations as a function of time.

* Further details of the experimental arrangements and of the results are given in the thesis of one of us.¹⁰

IV. ANALYTICAL

Two samples of usually 2 ml were taken from the electrolyte solution at suitable intervals. One sample served for the determination of the chloride ion concentration by a conventional titration method using silver nitrate as titrant and potassium bichromate as indicator. In the second sample the sum of the concentrations of hypochlorite, hypochlorous acid and molecular chlorine and the concentration of chlorate were determined using an improved potentiometric titration method, based on a procedure given by Norkus and Prokopchik.¹⁵ These authors determined hypochlorite by potentiometric titration with As_2O_3 . The chlorate was then reduced by excess As_2O_3 by heating the sample for several minutes to $90^\circ C$ after OsO_4 has been added as catalyst. The excess arsenic oxide was titrated with potassium bromate solution using methyl orange as indicator (cf. Peters and Deutschländer¹⁶).^{*} In our experiments the following procedure was found to give rapid and sufficiently accurate results: After the addition of some 1N sodium bicarbonate solution to the sample, hypochlorite was titrated potentiometrically with a solution of usually 0.05 or 0.005 M/lit As_2O_3 . A 100 ml beaker containing a

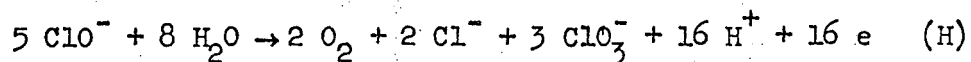
* Norkus and Prokopchik give a procedure by which ClO_2^- can be determined in the same sample. Hypochlorite is then titrated in alkaline medium, chlorite in neutral medium with OsO_4 as catalyst. The complete determination of hypochlorite, chlorite and chlorate was found by us to be rather uncertain and lengthy, because of the slowness of potential changes in alkaline medium. The determination of chlorite was not necessary, however, in our experiments, since tests showed that in chlorate electrolysis chlorite is never present in measurable amounts.

platinum ring electrode and a calomel electrode with ceramic double diaphragm was used. Before each run the platinum electrode had been immersed in conc. sulfuric acid containing chromate for a short moment. After reaching the hypochlorite endpoint excess arsenic oxide was added, then some potassium bromide (about 30 mg) and a volume of chemically pure concentrated hydrochloric acid approximately equal to the solution volume already present. The solution which had to contain now at least 20% HCl was then allowed to stand for 3 to 5 minutes. After that time the excess As_2O_3 was titrated potentiometrically with $KBrO_3$. The relative potential change was followed using a potentiometer range of 0-140 mV. The shape of the potentiometric titration curves is illustrated in Fig. 6. The accuracy of the chlorate concentration values determined by the described method was better than $\pm 2\%$ for chlorate concentrations not smaller than 0.001 M/lit. In view of its great importance for the present study the analytical procedure was tested in some detail. A more complete report of the experiments carried out has been given elsewhere.¹⁰

V. EXPERIMENTAL RESULTS

In each run the change of the hypochlorite concentration with time was followed, until a steady state with a constant hypochlorite concentration was reached (Fig. 2). The values of the hypochlorite concentrations and of the rates of chlorate formation measured in the steady state with dilute NaCl solutions are summarized in Table I. Measured and calculated rates of chlorate formation are compared in Table II in terms of the corresponding hypochlorite fluxes at the anode.

The linking of the rate of chlorate formation with the hypochlorite flux at the anode requires the knowledge of the stoichiometry of the anodic chlorate formation. According to reaction (F) three moles of hypochlorite, oxidized anodically, yield one mole of chlorate. Stoichiometric ratios different from those given by reaction (F) have been found by Rius and Llopis.^{17,18} According to these authors their experiments fit best the equation:



In this case only 1.7 moles of hypochlorite are needed to yield one mole chlorate. It seems that reaction (F) applies to acid baths, reaction (H) to strongly alkaline solutions. The great influence of pH on the stoichiometry of the anodic chlorate formation is apparent from Foerster's results² as well as from those of Rius and Llopis.^{17,18} It was also observed in a series of stoichiometric measurements carried out in our laboratory. Now, we have seen that with the model discussed in Section 2 the pH at the interface is quite low. We therefore use the stoichiometric ratios given by reaction (F). The formation of one mole chlorate then

corresponds to the diffusion of three moles of hypochlorite to the anode.

We thus have $j_e = 3v_{\text{ClO}_3}$, where v_{ClO_3} is the measured rate of chlorate formation (moles $\text{cm}^{-2}/\text{s}^{-1}$). We will regard j_e as an experimental value of the hypochlorite flux at the interface.

The hypochlorite flux for a diffusion controlled process (without influence of a chemical reaction) may be calculated from the bulk concentration c_o by:

$$j_d = -D_3 \frac{c_o}{\delta}$$

For the case that mass transfer is coupled with a first order chemical reaction (chlorine hydrolysis) the hypochlorite flux at the anode j_h is related to the bulk concentration by Eq. (8). In the calculation of j_d and j_h the diffusion coefficient of hypochlorite was assumed as $10^{-5} \text{ cm}^2/\text{s}$ since no measured values were available in the literature. The value of the rate constant for chlorine hydrolysis at 7°C was interpolated from an Arrhenius plot given in Ref. 14 as $k = 3.6 \text{ s}^{-1}$. The diffusion layer thickness was evaluated experimentally by measuring limiting currents for the reduction of ferricyanide to ferrocyanide at various flow rates. The measurements were performed at 25°C with a solution containing 0.05 M/lit potassium ferricyanide, 0.01 M/lit potassium ferrocyanide and 1.0 M/lit potassium chloride. The cell geometries and electrodes were the same as in the chlorate experiments. Figure 7 shows Nusselt numbers calculated from the measured limiting currents according to:

$$\text{Nu} = \frac{i_g L}{F c_{\text{Fe}} D_{\text{Fe}}}$$

as a function of the Reynolds number $\text{Re} = uL/v$, where i_g = limiting

current density; L = length of electrode* (here always 20 cm); F = Faraday constant; c_{Fe} = concentration of ferricyanide; D_{Fe} = diffusion coefficient of ferricyanide in 1N-KCl at 25°C equal to 0.7 cm²/sec;¹⁹
 u = linear flow velocity; ν = kinematic viscosity of the solution (equal to 0.85 cm²/s for 1 N KCl.²⁰

From Fig. 7 average thicknesses of the diffusion layer were calculated for chlorate experiments of corresponding Reynolds numbers, according to $\delta = L/Nu$. In the evaluation of Re the kinematic viscosity of a 0.05 N-sodium chloride solution at 7°C was taken as 1.42 cm²/s.^{20,21}

* For fully developed channel flow the quantity $L^* = 4 \frac{\text{cross section}}{\text{perimeter}}$ would be more appropriate in forming the dimensionless numbers Nu and Re than the quantity L which is used in describing the flow past a flat plate. Since in the chlorate experiments the ratio electrode area/electrolyte volume had to be not too small, the entrance length in our experiments was usually shorter than that required for the two hydrodynamic boundary layers to merge. The calculated value of the average diffusion layer thickness is not affected by the choice of the characteristic length as long as only experiments performed under equal geometrical conditions are compared as it was done here.

VI. DISCUSSION OF RESULTS

Table II shows that the ratio j_e/j_d strongly varies with the conditions and is always much larger than 1. The experimental rate of chlorate formation is up to 64 times larger than the value calculated for transport control without influence of a chemical reaction. This confirms our earlier results^{8,11} and is strong evidence that under the conditions of the experiments in Table I the rate of anodic chlorate formation is not controlled by simple mass transport of hypochlorite by diffusion and convection from the bulk to the anode.* The calculation considering the influence of the chlorine hydrolysis in the diffusion layer, on the other hand, fits the experimental results much better; the ratio j_e/j_h remains nearly constant and is close to 1, except for very high flow rates. This departure from the value 1 observed at high flow rates is not surprising, however. In the fundamental differential equation for the mass transport (Eq. 1) the convection term was dropped before carrying out the integration which finally yielded the relationship

* Mass transfer due to migration, although not entirely negligible in some of the experiments, played a minor role, since always excess chloride was present in the solution. Also the uncertainty in the assumption of a value of the diffusion coefficient does not alter the conclusions, since the uncertainty is expected to be smaller than a factor of 2 whereas j_d and j_h differ by an order of magnitude. Furthermore, if the estimated value of D was wrong, j_e/j_d would be different from 1 but would be constant in a transport controlled process.

giving j_h (Eq. 8). This procedure can lead to a good approximation only if the thickness δ_R of the zone in which the hydrolysis takes place (reaction layer) is small as compared to the normal thickness which the diffusion layer would have in the absence of a chemical reaction. Let us consider as representative for δ_R the distance from the anode at which the chlorine concentration has dropped to 1% of its value at the interface.* With $k = 3.6 \text{ s}^{-1}$ we obtain for this distance (from Eq. 3) a value of 3.8×10^{-3} cm. At flow rates of 13 and 44 cm/s this is smaller than the normal thickness of the diffusion layer δ , but not at flow rates of 145 and 154 cm/s (Tables I and II). These two latter flow rates are precisely those at which the ratio j_e/j_h becomes substantially larger than 1.

* The definition of the thickness of the reaction layer is somewhat arbitrary. One can also define an effective thickness of the reaction layer in a way quite similar to the definition of the usual effective or equivalent thickness of the adhering diffusion layer of Nernst. From Eq. (3) it can be easily derived that the effective thickness of the reaction layer is equal to $0.5 \sqrt{D_1/k}$ if the influence of convection is entirely disregarded. With $D = 10^{-5} \text{ cm}^2 \text{ s}^{-1}$ and $k = 3.6 \text{ s}^{-1}$ this effective thickness is about 2×10^{-3} cm. Comparison with the values of δ shown in Table II leads to the same conclusion as above, i.e. that the departure of j_e/j_h takes place at flow rates which appear as very reasonable from the viewpoint of the simplifications made.

From all this we can conclude that the model involving the coupling of mass transfer with a first order chemical reaction proceeding in the diffusion layer describes adequately the mechanism of anodic chlorate formation under the conditions of the experiments of Table I and Table II. In dilute NaCl solutions the rate of the anodic chlorate formation is governed by the kinetics of the chlorine hydrolysis in the immediate vicinity of the electrode.

In concentrated NaCl solutions, however, the ratio j_e/j_h is systematically substantially smaller than 1,²³ and, as we have seen in Fig. 1, the steady state bulk concentration of hypochlorite is much larger than in dilute solutions. This suggests that the mechanism of chlorate formation is not the same in dilute and concentrated NaCl solutions: The model developed in this paper appears to be restricted to dilute solutions. This can be readily understood by considering the chemical equilibrium of reaction (C) in the diffusion layer.* For the purpose of illustration the equilibrium HOCl concentration at the point where the HOCl concentration reaches a maximum in the diffusion layer, is calculated for the two experiments A and B listed in Fig. 2 and Table III. The bulk hypochlorite concentration is assumed to be zero in both cases. The distance from the anode at which the maximum is located, is obtained by differentiating Eq. (7) and setting $dc_3/dx = 0$:

* The outlined considerations based on the dependence of the rate of the chlorine hydrolysis and of the hydrolysis equilibrium in the diffusion layer on chloride concentration and pH may explain why there has to be a difference in the bulk hypochlorite concentration in dilute and concentrated chloride solutions. But there are also differences between the two cases with respect to the electrode reactions which will be discussed elsewhere.²³

$$X_m = \frac{1}{a} \ln Z$$

with

$$Z = \frac{1}{a\delta} (1 - e^{-a\delta}) - \frac{2 c_0 D_3 F}{\delta i\phi_1}$$

The corresponding numerical values are $X_m = 2.18 \times 10^{-3}$ cm for A and 2.49×10^{-3} cm for B. The hydrogen ion concentrations at X_m are 25.89×10^{-3} M/lt for A and 19.98×10^{-3} M/lt for B, calculated from Eq. (6), setting $\phi_2 = 1 - \phi_1$ and $D_2 = 5 \times 10^{-5}$ cm²/sec. The equilibrium concentration of HOCl is given by:

$$(\text{HOCl})_{\text{eq}} = \frac{K(\text{Cl}_2)}{(\text{Cl}^-)(\text{H}^+)}$$

where $K \approx 3 \times 10^{-4}$ M²/lt² at the temperature of the experiments.²² Setting for the chlorine concentration the maximum possible value corresponding to the saturation concentration $(\text{Cl}_2)_{\text{sat}} \approx 0.06$ M/lt one obtains the maximum possible values of the HOCl equilibrium concentration at X_m :

$$c_3 \text{ eq} = 0.17 \times 10^{-6} \text{ M/cm}^3 \quad (\text{A})$$

$$c_3 \text{ eq} = 16.1 \times 10^{-6} \text{ M/cm}^3 \quad (\text{B})$$

These concentrations may then be compared to the concentrations at X_m calculated from Eq. (7) for a first order irreversible reaction:

$$c_{3h} = 3.69 \times 10^{-6} \text{ moles/cm}^3 \quad (\text{A})$$

$$c_{3h} = 3.88 \times 10^{-6} \text{ moles/cm}^3 \quad (\text{B})$$

Comparison shows that for the dilute sodium chloride solution (experiment B) the value c_{3h} lies well below the equilibrium value. In concentrated sodium chloride solution (experiment A), on the other hand, the value of

c_{3h} is about 20 times larger than the equilibrium value. The above comparison illustrates the fact that in concentrated NaCl solutions the chlorine hydrolysis cannot proceed in the diffusion layer in the same way as in dilute solutions, because the equilibrium value is reached much earlier and the hydrolysis is therefore stopped. Our study of the concentrated solutions will be reported in more detail* in a subsequent paper.²³

Acknowledgements

The authors wish to thank A. Frei for helpful discussions. This work was supported by the Robert Gnehm Fonds of the Swiss Federal Institute of Technology and the Schweizerischer Aluminium Fonds, Zurich, and also by the United States Atomic Energy Commission.

* A summary of the results obtained with dilute and concentrated solutions has been recently given elsewhere.²⁴

Table I. Constant Current Electrolysis of Dilute NaCl Solutions Under Forced Convection

No.	Cl^- (M/Lt)	Tz (°C)	pH	u (cm/sec)	i (mA/cm ²)	E_A (mV v. SCE)	Gap Width (mm)	c_{st} (mM/Lt)	v_{ClO_3} (M/cm ² sec $\times 10^{-9}$)	τ_{ClO_3} (%)
1	0.046	0.0	4.0	13	1	1580	9	1.95	0.93	53.7
2	0.055	0.0	1.9	13	1	1560	9	1.50	0.72	41.6
3	0.037	3.2	3.1	13	5	1620	9	5.4	3.56	41.2
4	0.047	0.3	9.0	13	5	1600	9	6.4	4.30	49.8
5	0.130	2.2	9.0	13	5	1580	9	14	5.41	62.7
6	0.047	7.8	2.0	13	5	1580	9	1.4	3.32	38.4
7	0.052	7.0	2.0	13	5	1610	9	0.5	1.72	19.8
8	0.05	7.0	9.0	13	5	1680	9	1.0	2.07	23.9
9	0.05	7.0	9.0	13	5	1670	9	1.6	2.94	34.0
10	0.05	7.0	9.0	13	5	1660	9	1.2	2.87	33.2
11	0.1	7.0	9.0	13	10	1720	9	3	7.11	41.0
12	0.073	7.0	9.0	44	5	1530	9	1.3	3.39	39.2
13	0.053	7.0	9.0	44	5	1550	9	0.3	1.71	19.7
14	0.083	7.0	9.0	44	5	1580	9	1.0	2.84	32.8
15	0.052	7.0	2.0	44	5	1610	9	0.8	2.70	31.2
16	0.052	7.0	2.3	154	5	1700	2.25	0.4-0.3	2.01	23.3
17	0.055	7.0	2.1	154	5	1740-1900	2.25	(0.2)	1.77	20.4
18	0.053	7.0	9.2	153	5	1700	2.25	0.3-0.25	2.35	27.2
19	0.1	7.0	9.0	145	10	1810	2.25	0.7	6.06	35

Cl^- : Average value of chloride concentration in the steady state. The chloride concentration was held constant by adding conc. HCl periodically. Tz: Average cell temperature. Variations in cell temperature with time $\leq \pm 0.5^\circ$. pH: During the experiment the pH could vary ± 0.3 due to the automatic regulation. u: Linear flow velocity. i: Current density. E_A : Steady state anode potential. Given values are rounded average values, since the potentials were not always constant during an experiment. gap width: Distance between anode and diaphragm. c_{st} : Measured total steady state concentration of hypochlorite hypochlorous acid and chlorine. v_{ClO_3} : Chlorate formation rate in the steady state determined from the slope of chlorate concentration vs time curves. τ_{ClO_3} : Current efficiency of chlorate formation related to the reaction $Cl^- \rightarrow Cl^{5+} + 6e$ (6F per mol $ClO_3^- = 100\%$).

Table II. Comparison Between Measured and Calculated Chlorate Formation Rates

No.	δ ($\text{cm} \times 10^{-2}$)	c_o (M/cm^3) ($\times 10^{-6}$)	j_e ($\text{M}/\text{cm}^2 \text{ sec}$) ($\times 10^{-9}$)	j_d ($\text{M}/\text{cm}^2 \text{ sec}$) ($\times 10^{-9}$)	j_h ($\text{M}/\text{cm}^2 \text{ sec}$) ($\times 10^{-9}$)	j_e/j_d	j_e/j_h
1	1.8	1.95	2.79	1.08	3.49	2.6	0.8
2		0.47	2.16	0.26	2.13	8.3	1.0
3		4.5	10.68	2.50	11.74	4.3	0.9
4		6.4	12.90	3.55	14.71	3.6	0.9
5		14	16.23	7.78	21.82	2.1	0.7
6		0.42	9.96	0.23	9.27	43.3	1.1
7		0.14	5.16	0.08	4.76	64.5	1.1
8		1.0	6.21	0.56	6.19	11.1	1.0
9	0.74	1.6	8.82	0.89	8.89	9.9	1.0
10		1.2	8.61	0.67	8.48	12.9	1.0
11		3.0	21.33	1.67	21.02	12.8	1.0
12		1.3	10.17	1.76	9.66	5.8	1.1
13		0.3	5.13	0.41	4.40	12.5	1.2
14		1.0	8.52	1.35	7.97	6.3	1.1
15		0.22	8.10	0.30	6.60	27.0	1.2
16	0.24	0.08	6.03	0.33	3.16	18.3	1.9
17		0.05	5.31	0.21	2.70	25.3	2.0
18		0.25	7.05	1.04	4.35	6.8	1.6
19	0.26	0.70	18.18	2.69	11.63	6.8	1.6

δ Average thickness of diffusion layer, calculated from limiting current measurements for ferricyanid reduction.

c_o Concentration of hypochlorite and hypochlorous acid in the steady state. c_o is related to the total concentration of chlorine, hypochlorous acid and hypochlorite c_{st} by

$$c_o = \frac{K_1 c_{st}}{(\text{Cl}^-)(\text{H}^+) + K_1} \times 10^{-3} \quad [\text{M}/\text{cm}^3]$$

where K_1 is the equilibrium constant of the chlorine hydrolysis

$$K_1 = \frac{(\text{HOCl})(\text{Cl}^-)(\text{H}^+)}{(\text{Cl}_2)} \quad \text{in} \quad \text{M}^2/\text{Lt}^2$$

j_e Hypochlorite flux at the anode determined from experimentally measured chlorate formation rates: $j_e = 3\nu\text{ClO}_3$ [cf. Reaction (F)].

j_d Hypochlorite flux at anode calculated from steady state hypochlorite concentration assuming a diffusion controlled process: $j_d = -D_3 c_o/\delta$

j_h Hypochlorite flux at anode calculated by taking into consideration the chlorine hydrolysis within the diffusion layer [Equation (8)].

Table III. Data of Experiments A and B Used in the Calculation of Concentration Profiles and Equilibrium Concentrations

	A	B
Sodium chloride concentration (M/Lt)	4.0	0.056
Current density (mA/cm ²)	20	20
Average temperature (°C)	20	13
Average pH	9.3	9.0
Steady state hypochlorite concentration (M/Lt)	134	10
Steady state chlorate formation rate (M/cm ² sec)	20×10 ⁻⁶	17.6×10 ⁻⁶
Current efficiency for chlorate formation (%)	57.8	50.8
Thickness of diffusion layer (cm) calculated from oxygen evolution rate	1.1×10 ⁻²	0.9×10 ⁻²

REFERENCES

1. F. Foerster, *Elektrochemie wässriger Lösungen*, 3. Aufl. (1922).
2. F. Foerster, *Trans. Am. Electrochem. Soc.* 46, 23 (1924).
3. E. Müller, *Z. Elektrochemie* 5, 469 (1899).
4. N. V. S. Knibbs and H. Palfreeman, *Trans. Faraday Soc.* 16, 402 (1920).
5. V. de Valera, *Trans. Faraday Soc.* 49, 1338 (1953).
6. T. Beck, paper presented at the Spring Meeting of the E.C.S. in Indianapolis, May 1961.
7. L. Hammar and G. Wranglén, *Electrochimica Acta* 9, 1 (1964).
8. A. Selvig, *thésis ETH, Zurich, Prom. Nr. 3268* (1962).
9. N. Ibl and J. Venczel, paper presented at the Cleveland Meeting of the E.C.S., April 1966; J. Venczel, *thesis ETH, Zurich, Prom. Nr. 3019* (1961).
10. D. Landolt, *thesis ETH, Zurich, Prom. Nr. 3673* (1965).
11. N. Ibl, *Chem. Ing. Techn.* 35, 353 (1963).
12. T. Beck and N. Ibl, unpublished correspondence (1962/63).
13. J. W. Ingham and J. Morrison, *J. Chem. Soc.* 8, 1200 (1933).
14. C. W. Spalding, *A.I.Ch.E.* 8, 685 (1962).
15. P. K. Norkus and A. Yu. Prokopchik, *Zhur. Anal. Khim* 16, 336 (1961).
16. K. Peters and E. Deutschländer, *Apoth. Z.* 594 (1926).
17. A. Rius and J. Llopis, *Anales Fisica y Quimica* 41, 1030, 1282, 1395 (1945).
18. J. Llopis, *Anales Fisica y Quimica* 42, 41 (1946).
19. D. Jahn and W. Vielstich, *J.E.C.S.* 109, 849 (1962).
20. Handbook of Chemistry and Physics, D. C. Hodgman, R. C. West and S. M. Selby, Editors (Chemical Rubber Publ. Co., Ohio, 1961), 43rd edition.

21. Landolt-Börnstein, Phys. Chem. Tab. 1, 138 (1923).
22. R. E. Connick and Y. T. Chia, J. Am. Chem. Soc. 81, 1280 (1959).
23. D. Landolt and N. Ibl, to be published in Electrochimica Acta.
24. N. Ibl and D. Landolt, Chem. Ing. Tech. 39, 706 (1967).

FIGURE CAPTIONS

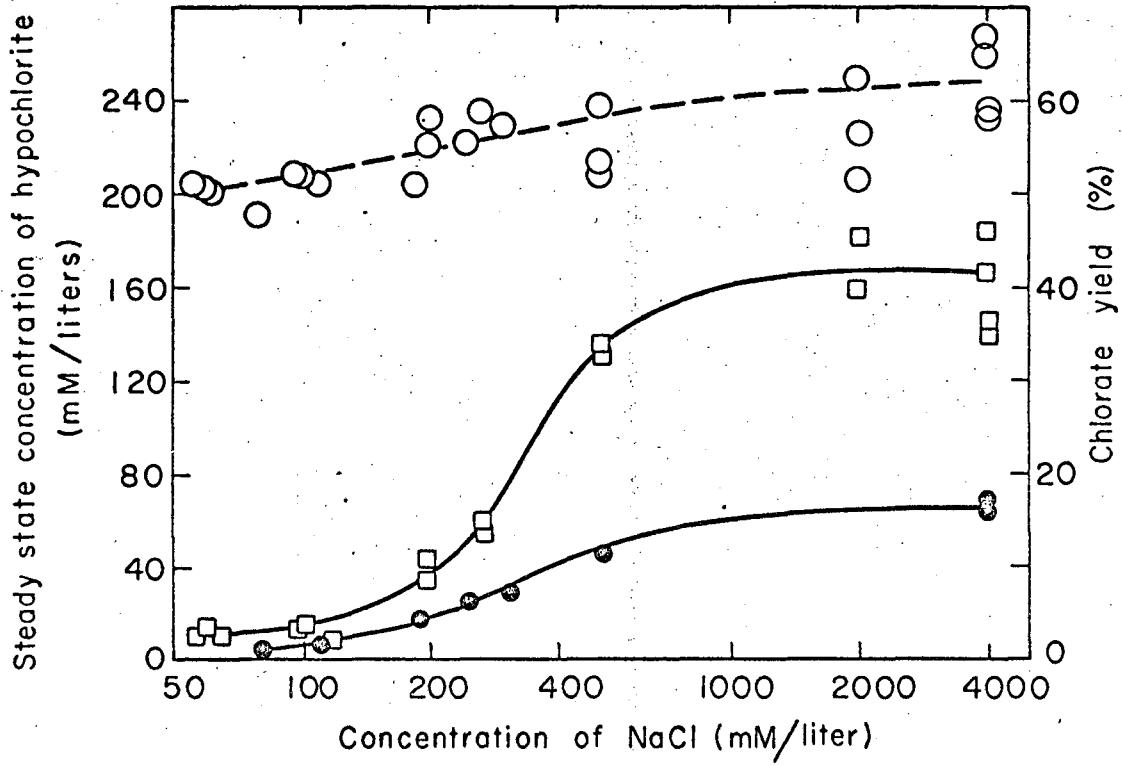
- Fig. 1 Steady state hypochlorite concentrations and chlorate formation rates at various chloride concentrations in stagnant solutions.
- hypochlorite concentration $i = 5\text{mA/cm}^2$
 - hypochlorite concentration $i = 20\text{mA/cm}^2$
 - chlorate yield $i = 5\text{mA/cm}^2$, $i = 20\text{mA/cm}^2$
- Fig. 2 Variation of hypochlorite and chlorate concentration with time during electrolysis of NaCl solution.
- concentration of NaCl = 4 M/lt
 - concentration of NaCl = 0.05 M/lt, maintained approximately constant during experiment.
- Fig. 3 Concentration profiles near the anode (schematically).
- Fig. 4 Calculated hypochlorite concentration profiles in the diffusion layer (experiment B).
- | | | | |
|-----------|--|---|---|
| Curve I | $c_o = 10 \times 10^{-6} \text{ M/cm}^3$ | } | Diffusion coupled with
chemical reaction |
| Curve II | $c_o = 0$ | | |
| Curve III | Diffusion controlled process, $c_o = 10 \times 10^{-6} \text{ M/cm}^3$ | | |
- Fig. 5a Experimental set-up for continuous flow electrolysis. A: anode, B: bulk reservoir, C: cathode, D: diaphragm, E: reference electrode, F: backside capillary, G: gas outlet, L: cooling device, M: buret for automatic pH control, N: pressure compensating tube, P: pump, R: rotameter, S: channels for quieting the flow, T: thermometer, W: gas washing bottle, Z: glass electrode.

Fig. 5b Flow Cell. For caption see Fig. 5a.

Fig. 6 Potentiometric titration of hypochlorite and chlorate.

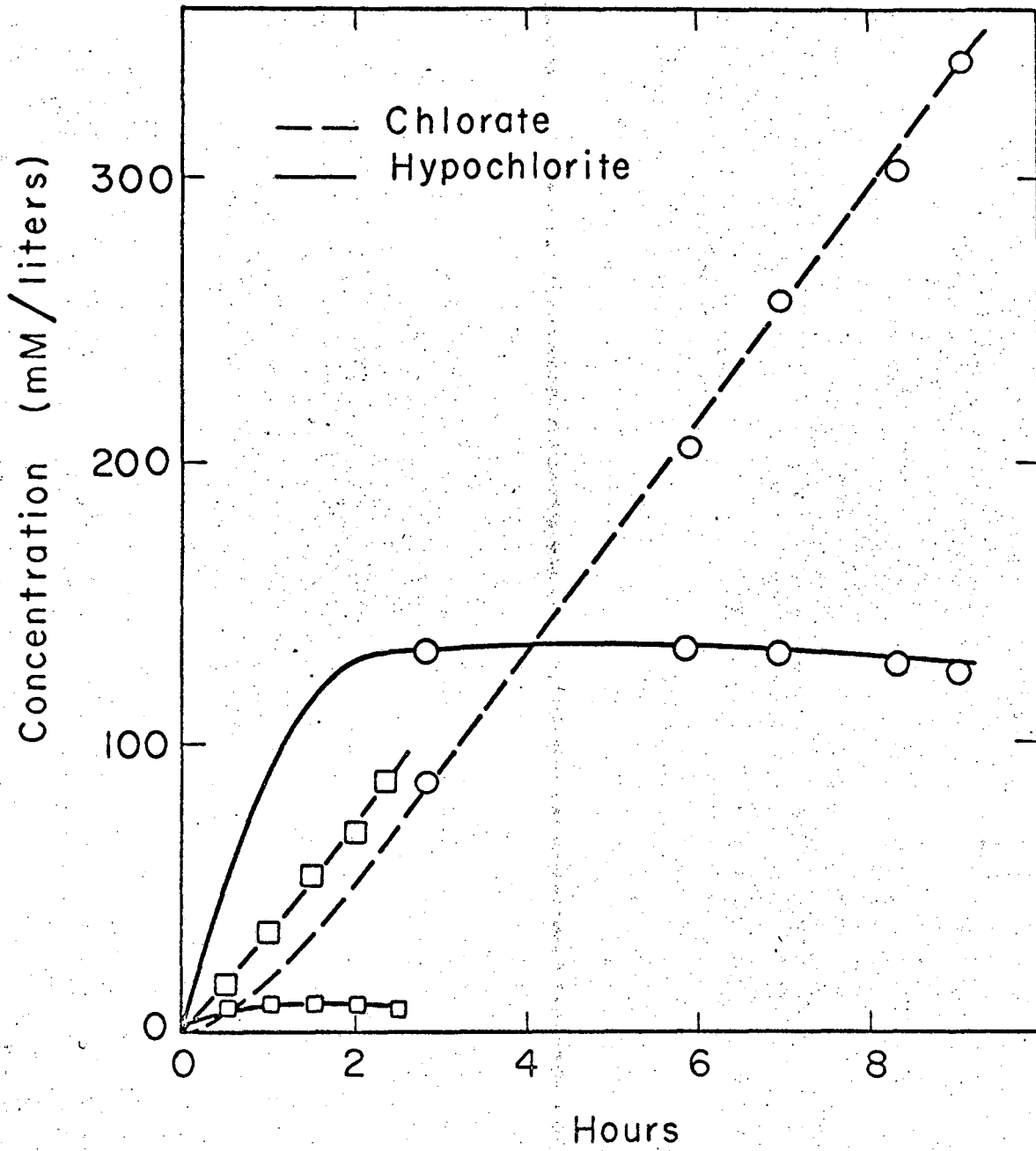
Fig. 7 Evaluation of mass transfer conditions in flow cell by measuring limiting current for the reduction of ferricyanide.

• gap width 9 mm, + gap width 2.25 mm.



XBL673-2427

Fig. 1



XBL673-2428-A

Fig. 2

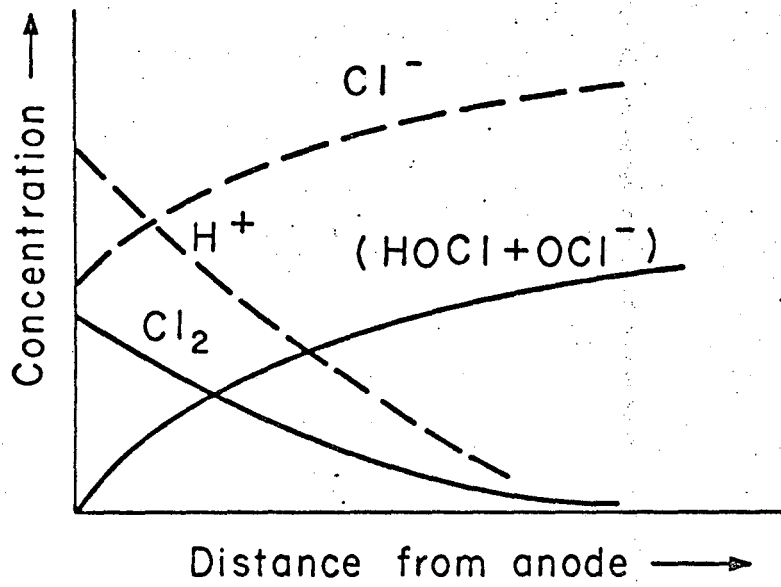
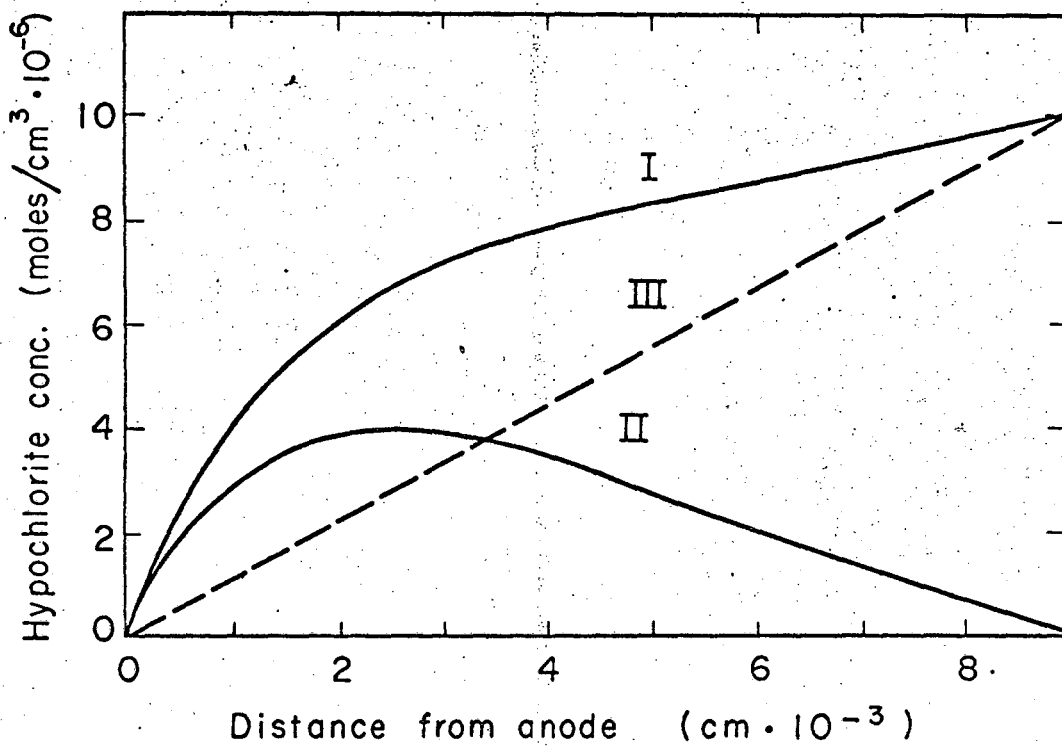


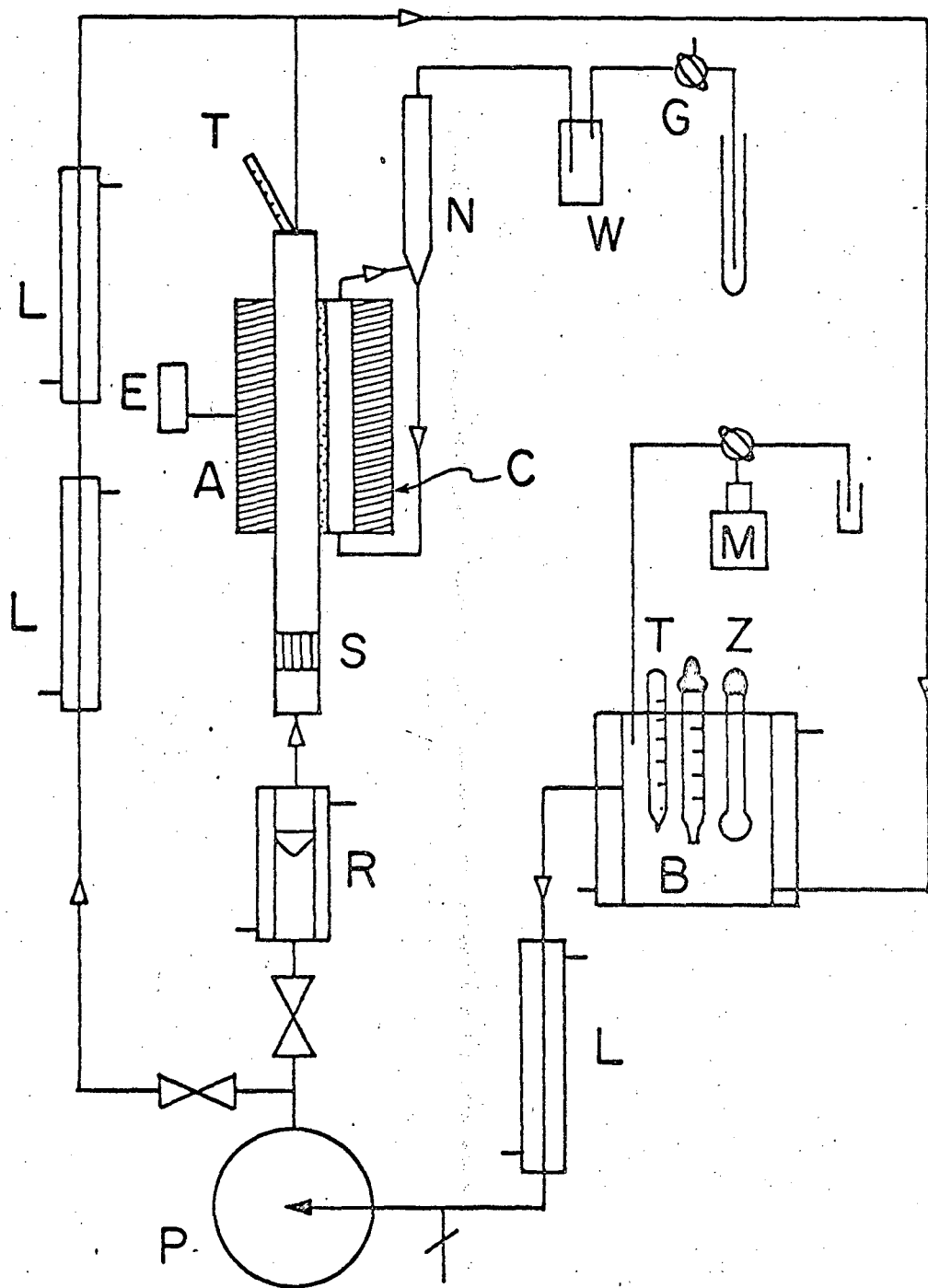
Fig. 3

XBL673-2429



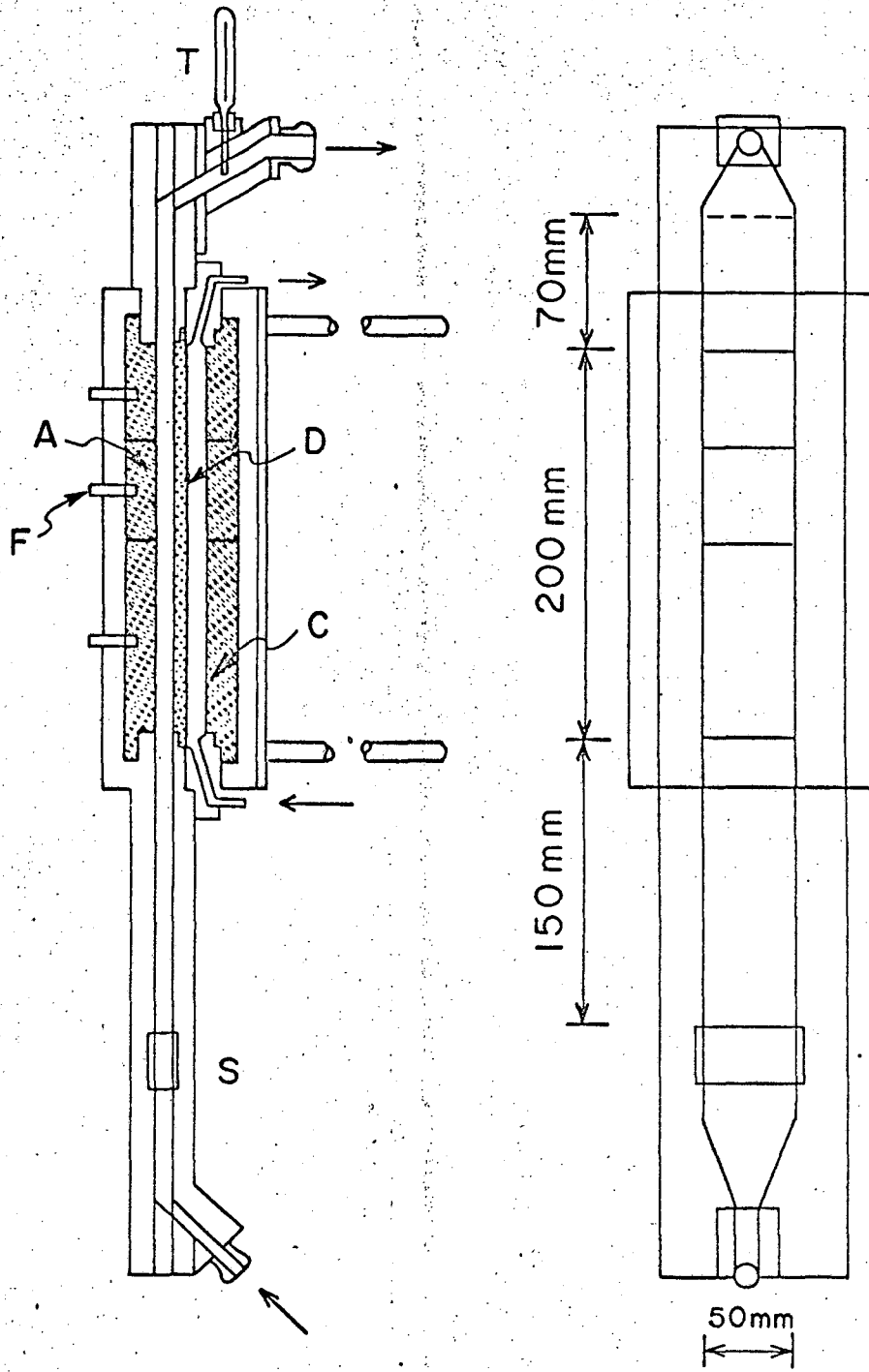
XBL673-2430-A

Fig. 4



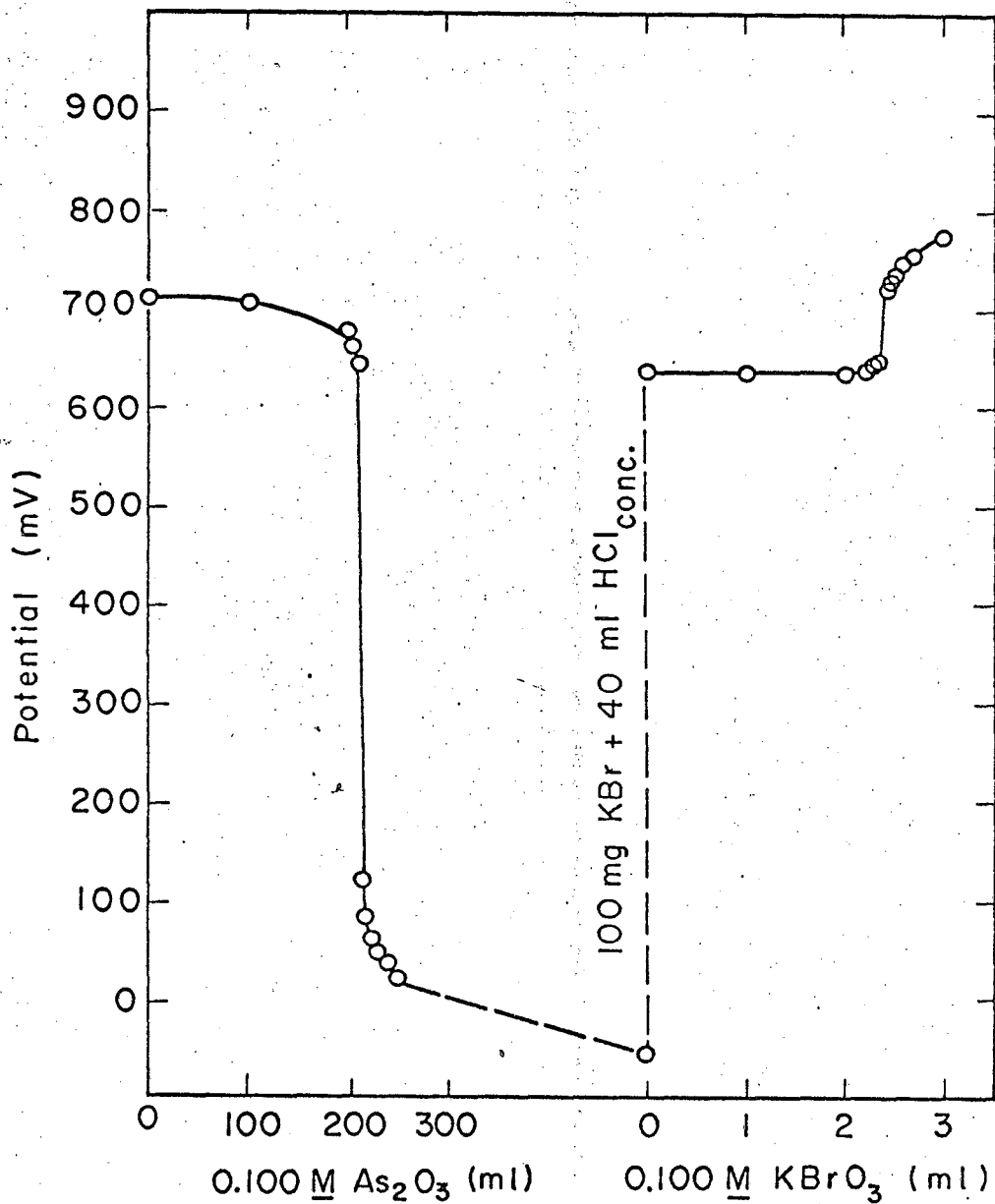
XBL673-2431-A

Fig. 5a



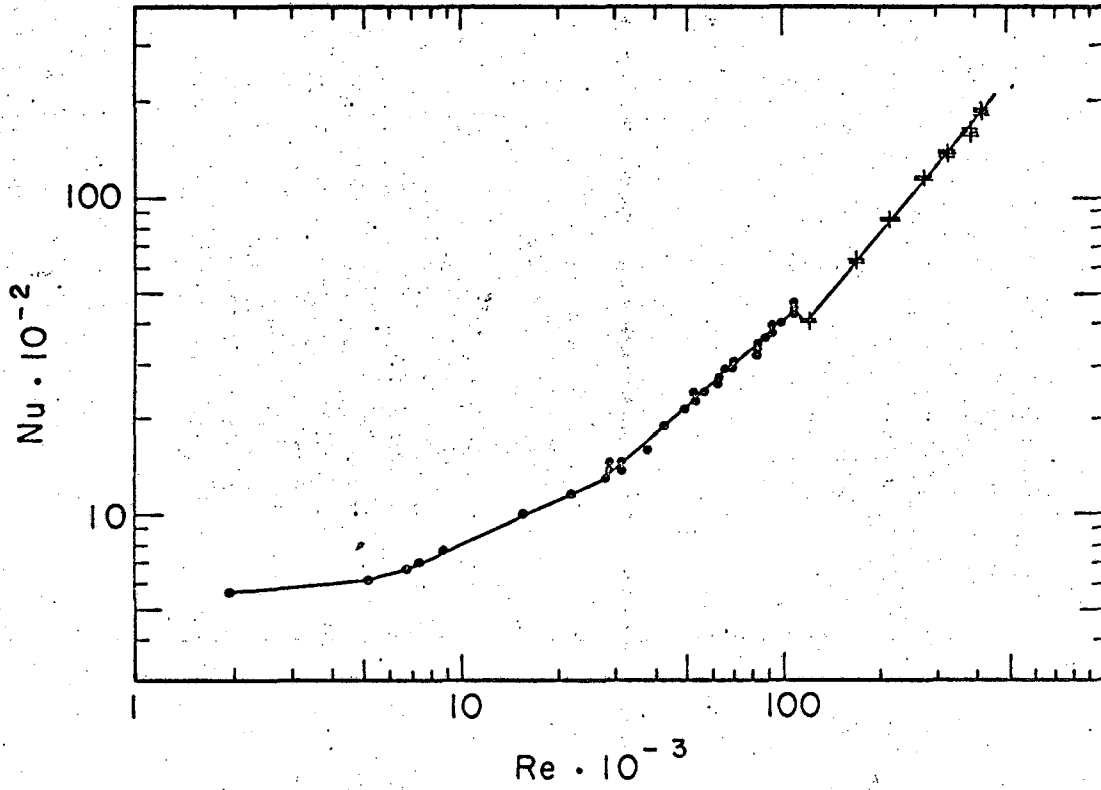
XBL673-2432-A

Fig. 5b



XBL673-2433

Fig. 6



XBL673-2434

Fig. 7

This report was prepared as an account of Government sponsored work. Neither the United States, nor the Commission, nor any person acting on behalf of the Commission:

- A. Makes any warranty or representation, expressed or implied, with respect to the accuracy, completeness, or usefulness of the information contained in this report, or that the use of any information, apparatus, method, or process disclosed in this report may not infringe privately owned rights; or
- B. Assumes any liabilities with respect to the use of, or for damages resulting from the use of any information, apparatus, method, or process disclosed in this report.

As used in the above, "person acting on behalf of the Commission" includes any employee or contractor of the Commission, or employee of such contractor, to the extent that such employee or contractor of the Commission, or employee of such contractor prepares, disseminates, or provides access to, any information pursuant to his employment or contract with the Commission, or his employment with such contractor.

